A Reaction Kinetic Mechanism for Methane Hydrate Formation in Liquid Water

Knut Lekvam*,† and Peter Ruoff*,‡

Contribution from the Rogaland Research Institute, Box 2503 Ullandhaug, 4004 Stavanger, Norway, and Rogaland University Center, Box 2557 Ullandhaug, 4004 Stavanger, Norway

Received March 29, 1993®

Abstract: On the basis of experimental studies, we propose a reaction kinetic model for the formation of methane hydrate from liquid water and methane gas. The model consists of 5 pseudoelementary processes with the following three dynamic elements: (1) the dissolution of methane gas into the water phase, (2) the buildup of an oligomeric precursor of methane hydrate, and (3) the growth of methane hydrate by an autocatalytic process. The integrated rate equations of our model show close agreement to experimentally observed behavior.

Introduction

A variety of gases, among them the components of natural gas, form with water at low temperature and high pressure solid, crystalline clathrate compounds, so-called gas hydrates. In these hydrates the gas molecules are trapped in cages that consist of the host lattice water molecules. Although Davy described the chlorine (Cl_2) hydrate as the first gas hydrate at the beginning of the 19th century,[1] it was the discovery of natural gas hydrates as plugs in pipelines in the 1930's that initiated the first systematic studies.[2,3]

The structure and equilibrium thermodynamic properties of natural gas hydrates appear to be quite well understood,[4,5] and the attention of researchers is now being focused more toward understanding their kinetic properties. Previous kinetic studies investigated the formation rates of several gas hydrates[6–9] and their nucleation phenomena.[10] Falabella[11] showed that methane or krypton hydrates formed from ice show induction periods, while hydrates formed from ethane, acetylene, or carbon dioxide do not have induction periods.

Vysniauskas and Bishnoi[12] investigated the initial rate of methane hydrate formation from liquid water. These authors proposed a semiempirical model describing the initial rate as an explicit function of the surface area of the gas–water interface, the degree of supercooling, the activation energy, and the total gas pressure.

On the basis of constant pressure experiments with the same equipment as Vysniauskas and Bishnoi,[12] Englezos et al.[13] proposed a model for the macroscopic growth rates dependent on the supersaturation of water with gas at the onset of hydrate formation for methane and ethane and mixtures thereof.[14] Gas consumption up to as much as 40% in excess of the expected pseudo-two-phase equilibrium was reported.

Sloan and Fleyfel[15] recently suggested a kinetic model consisting of three consecutive processes to explain induction times in the formation of methane or krypton hydrates from ice.

We have studied the formation of methane hydrate in liquid water in a closed temperature-controlled reactor. In this paper we show typical dynamics observed during the stages when methane hydrate is being formed and propose a reaction kinetic mechanism. The mechanism consists of a set of pseudoelementary processes, which obey the principles of mass balance and microscopic reversibility. Our simulation calculations show close agreement with experimentally observed kinetics.

Materials and Methods

Experimental Details. A (transparent) sapphire cell was employed for the studies of the hydrates (Figure 1). The cell volume was 22 mL and it was pressure-tested up to 550 bar. However, for safety reasons, normal use was limited to a maximum pressure of 350 bar. The cell was placed into a thermostated water bath. The temperature inside the bath was automatically regulated by a program unit. During experiments, temperature variations inside the bath were ±0.03 °C. The thermostated bath was equipped with windows through which observations, photographs, and video recordings could be made. The cell was equipped with an externally driven magnetic stirring mechanism with a stainless steel paddle; the stirring rate was kept constant (1180 rpm) during experiments. Pressure and temperature were measured inside the cell with a Trafag 8832, 0–250 bar, pressure transmitter and a 1/10 DIN Pt-100 4-wire lead resistance element, respectively.

In all experiments double-distilled and degassed water and methane gas of 99.995% purity were used.

Prior to commencement of the hydrate-forming experiments, the sapphire cell was dismantled and thoroughly cleaned. Water was then added to the cell. The system was evacuated for a short while, followed by the addition of methane at a constant temperature outside the thermodynamic hydrate-forming region (Figure 2). Cell stirring was then switched on. The stirring was switched off after a few minutes by which time two-phase equilibrium had been achieved. The temperature was then lowered to a stable level at the desired experimental temperature. The cooling gradient was approximately 25 °C/h. After the target temperature was achieved, the bath temperature was overshot by a maximum of 0.3 °C before stabilizing permanently. The experiment was started by switching on the stirrer.

The Mechanistic Model. Our model consists of the following five pseudoelementary processes, which define the reactants ($CH_4(g)$, H_2O),

† Rogaland Research Institute.
‡ Rogaland University Center.
• Abstract published in *Advance ACS Abstracts*, August 15, 1993.

(1) Davy, H. *Philos. Trans. R. Soc.* **1811**, *101*, 1.
(2) Hammerschmidt, E. G. *Ind. Eng. Chem.* **1934**, *26*, 851.
(3) von Stackelberg, M. *Naturwissenschaften* **1949**, *37*, (a) 327, (b) 359.
(4) Finjord, J. *Hydrates of Natural Gas. A State-of-the-Art Study with Emphasis on Fundamental Properties*; Technical Report No. T11/83, Rogaland Research Institute: Stavanger, 1983.
(5) Sloan, E. D. *Clathrate Hydrates of Natural Gases*; Marcel Dekker: New York, 1990.
(6) Knox, W. G.; Hess, M.; Jones, G. E.; Smith, H. B. *Chem. Eng. Prog.* **1961**, *57*, 66.
(7) Barrer, R. M.; Stuart, W. I. *Proc. R. Soc. (London)* **1958**, *A243*, 172.
(8) Barrer, R. M.; Ruzicka, D. J. *Trans. Faraday Soc.* **1962**, *58*, 2262.
(9) Barrer, R. M.; Edge, A. V. J. *Proc. R. Soc. (London)* **1967**, *A300*, 1–24.
(10) Makogon, Y. F. *Hydrates of Natural Gas*; Moscow; PennWell: Tulsa, 1981.
(11) Fallabella, B. J. Ph.D. Thesis, University of Massachusetts, 1975.
(12) Vysniauskas, A.; Bishnoi, P. R. *Chem. Eng. Sci.* **1983**, *38*, 1061–1072.
(13) Englezos, P.; Kalogerakis, N.; Dholabhai, P. D.; Bishnoi, P. R. *Chem. Eng. Sci.* **1987**, *42*, 2647–2658.
(14) Englezos, P.; Kalogerakis, N.; Dholabhai, P. D.; Bishnoi, P. R. *Chem. Eng. Sci.* **1987**, *42*, 2659–2666.
(15) Sloan, D. E.; Fleyfel, F. *AIChE J.* **1991**, *37*, 1281–1292.

0002-7863/93/1515-8565$04.00/0

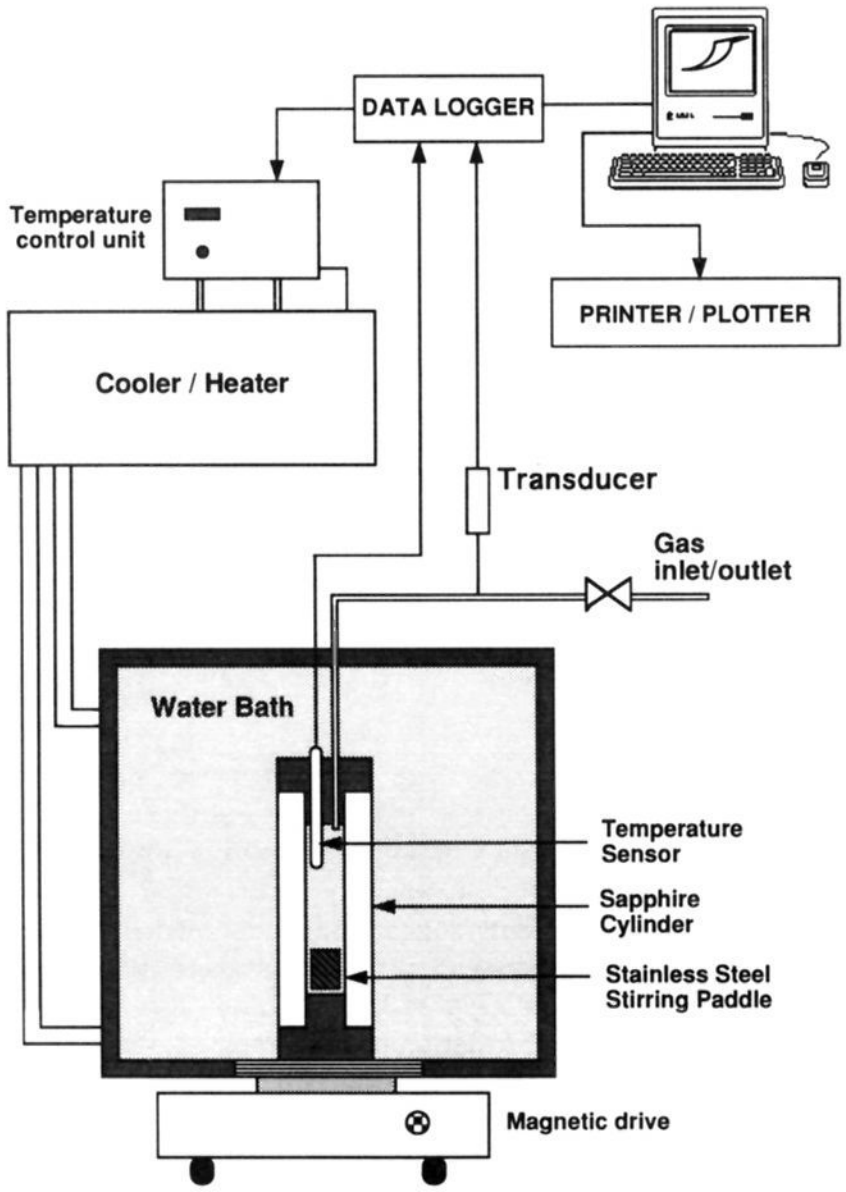

Figure 1. Schematic representation of the sapphire cell, temperature bath, and logging equipment.

product (hydrate species "H"), and reaction intermediates (dissolved methane, $CH_4(aq)$, and hydrate precursor species N):

$$CH_4(g) \underset{k_{-1}}{\overset{k_1}{\rightleftarrows}} CH_4(aq) \quad \text{(M1)}$$

$$f\cdot CH_4(aq) + h\cdot H_2O \underset{k_{-2}}{\overset{k_2}{\rightleftarrows}} N \quad \text{(M2)}$$

$$N \overset{k_3}{\rightarrow} H \quad \text{(M3)}$$

$$N \underset{k_{-4}}{\overset{k_4[H]}{\rightleftarrows}} H \quad \text{(M4)}$$

$$f\cdot CH_4(aq) + h\cdot H_2O \underset{k_{-5}}{\overset{k_5}{\rightleftarrows}} H \quad \text{(M5)}$$

The advantage of writing processes M1–M5 as pseudoelementary processes is that the rate equations can immediately be written down and solved mathematically.

Process M1 describes the dissolution of methane into the water phase. Reaction M2 describes the formation of oligomeric "precursors" N, while process M3 is a slow (uncatalyzed) formation of methane hydrate H from species N. The growth of methane hydrate H occurs due to the autocatalytic processes M4 and M5. While M4 describes the growth of methane hydrate crystals from preceding nuclei N, process M5 represents the formation of methane hydrate directly from the reaction between water and the dissolved gas.

Model Computations. Double-precision computations were performed on Sun SPARC stations and on Hewlett-Packard 9000/700 computers by integrating the rate equations from processes M1–M5 with the FORTRAN subroutine LSODE.[16] Table I shows the rate constant values and the stoichiometric factors "f" and "h" used in the computations. Origins of k_1–k_5, f, and h are discussed at the end of Computational Results.

(16) Hindmarsh, A. C. *ACM-SIGNUM Newsletter* **1980**, *15*, 10.

Table I. Rate Constant Values and Stoichiometric Factors Used in the Computations

$k_1 = 0.01341\ min^{-1}$	$k_{-1} = 0.449\ min^{-1}$
$k_2 = 1 \times 10^{-3}\ M^{1-f-h}\ min^{-1}$	$k_{-2} = 3.07 \times 10^{-3}\ min^{-1}$
$k_3 = 3 \times 10^{-1}\ min^{-1}$	
$k_4 = 1 \times 10^{10}\ M^{-1}\ min^{-1}$	$k_{-4} = 2.8 \times 10^{6}\ min^{-1}$
$k_5 = 1 \times 10^{9}\ M^{-f-h}\ min^{-1}$	$k_{-5} = 8.6 \times 10^{5}\ min^{-1}$
$f = 0.97$	$h = 5.75$

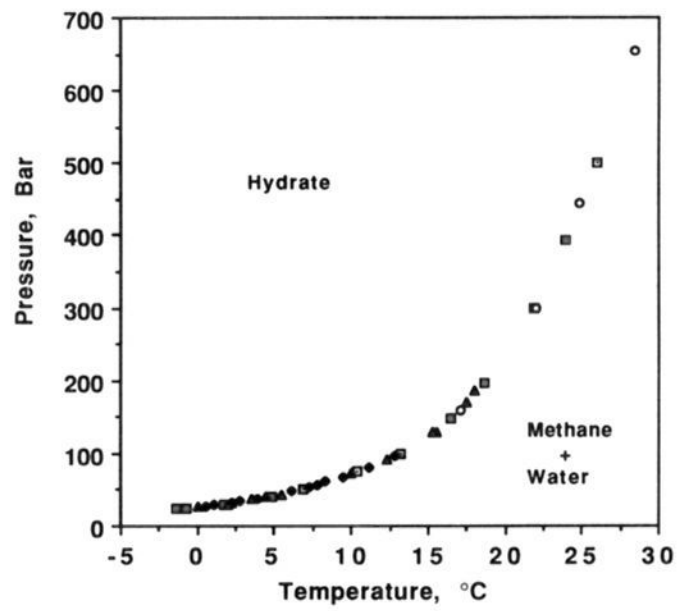

Figure 2. Pressure–temperature diagram for the methane–water system. Data points in the diagram represent the experimentally determined border which separates the thermodynamic conditions where methane hydrate may form or dissociate.[20]

Experimental Results

Nonreactive Dissolution of Methane in Water. The basis for these experiments is the assumption that methane is first dissolved into the water phase before further reaction steps can occur, i.e.,

$$CH_4(g) \underset{k_{-1}}{\overset{k_1}{\rightleftarrows}} CH_4(aq) \rightarrow \text{further reaction products} \quad \text{(R1)}$$

To obtain an estimate of the rate constants k_1 and k_{-1} without interference of further reaction steps, we studied the kinetics of the pressure drop when methane is stirred into the water *outside* the thermodynamic stability region of methane hydrate (Figures 2 and 3A).

Since in our experiments the amount of dissolved methane is always considerably less than the amount of water, the process

$$CH_4(g) \underset{k_{-1}}{\overset{k_1}{\rightleftarrows}} CH_4(aq) \quad \text{(M1)}$$

is expected to follow standard reversible pseudo-first-order kinetics with the following rate law:

$$\log\left(\frac{[CH_4]^t(g) - [CH_4]^\infty(g)}{[CH_4]^0(g) - [CH_4]^\infty(g)}\right) = -(k_1 + k_{-1})t \quad (1)$$

$[CH_4]^t(g)$ is the molar methane concentration in the gas phase at time t, where $[CH_4]^\infty(g)$ is the respective equilibrium value ($t = \infty$). Figure 3B shows that eq 1 is indeed followed with high precision and illustrates (together with Figure 3A) the determination of the rate constants k_1 and k_{-1}. The inset of Figure 3A displays the Arrhenius plots for the rate constants k_1 and k_{-1}. Table II contains the numerical values of k_1 and k_{-1} for a variety of temperatures and pressures and compares the equilibrium constant, $K = k_1/k_{-1}$, with values obtained from the Krichevsky and Kasarnovsky relation.[17]

From the Arrhenius plots, we were able to estimate the rate constants k_1 and k_{-1}. These estimates are used later in the model computations.

(17) Krichevsky, I. R.; Kasarnovsky, J. S. *J. Am. Chem. Soc.* **1935**, *57*, 2168.

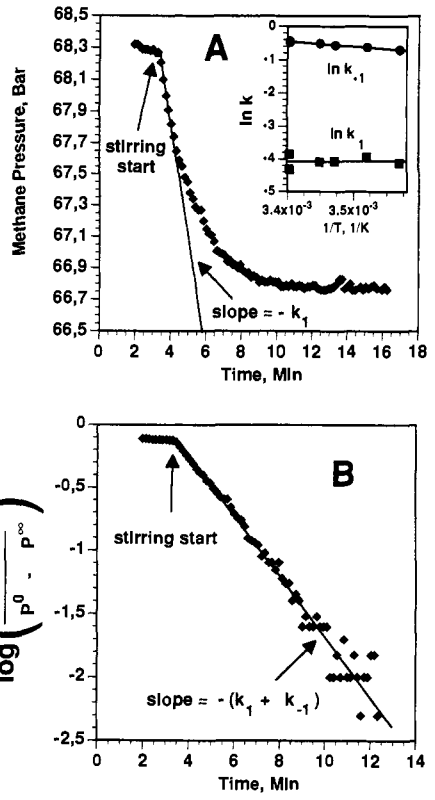

Figure 3. (A) Kinetics of the pressure drop when methane gas is stirred into the water phase. No methane hydrate is formed. Initial conditions: water, 14 g; temperature, 11.0 °C; initial amount of methane gas, 68.27 bar occupying 8 mL (0.023 mol). Inset: Arrhenius plot for determined rate constants k_1 and k_{-1} (see part B). Lines represent linear regression of data points. The determined activation energy for k_1 is zero, and the value for k_{-1} is 12.5 kJ/mol. (B) Plot showing that the unreactive stir-in of methane gas into the water phase follows reversible first-order kinetics.

Table II. Rate and Equilibrium Constants for the Nonreactive Methane Water System

temp, °C	k_1, min^{-1}	k_{-1}, min^{-1}	$K = \bar{k}_1/k_{-1}$[a]	K[b]
11.0	0.0159	0.4934	0.0349	0.0325
15.1	0.0194	0.5332	0.0323	0.0329
19.1	0.0170	0.5624	0.0307	0.0310
21.0	0.0167	0.5930	0.0291	0.0295
25.0	0.0172	0.6325	0.0273	0.0284

[a] $\bar{k}_1$ is the mean of the k_1 values. [b] Calculated with the Krichevsky and Kasarnovsky relation.[17]

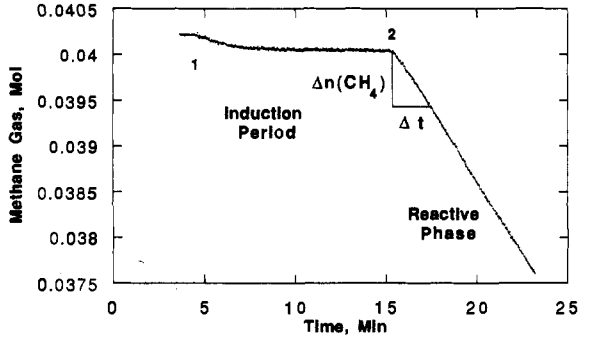

Figure 4. Induction period and reactive phase in the formation of methane hydrate from liquid water: (1) start of stirring; (2) end of induction period and beginning of reactive phase. $\Delta n(CH_4)/\Delta t$ defines the initial velocity of hydrate formation. Conditions: temperature, 6 °C; initial amount of water, 14 g; initial amount of methane, 0.0401 mol occupying a volume of 8 mL.

Reaction of Methane with Water. Figure 4 shows typical behavior in the pressure drop which is frequently encountered when the system is *inside* the region of the CH_4–H_2O phase diagram where hydrate is thermodynamically stable (Figure 2). Figure 4 shows that the methane hydrate formation in water can be divided into two main phases: (a) the induction period, and (b) the reactive phase.

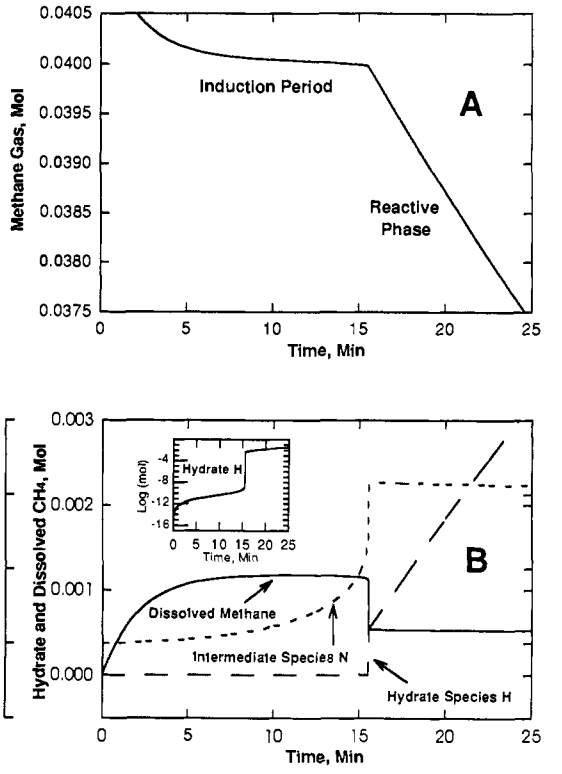

Figure 5. (A) Simulation calculation of a system similar to that of Figure 4. Conditions: initial amount of water, 14 g; initial amount of methane, 0.04124 mol. (B) Calculated amounts of intermediates of the reaction simulated in part A. The inset shows changes in the number of moles of hydrate species H by orders of magnitude during the induction period.

During the induction period the dissolved methane concentration is in a steady state. The methane pressure shows a slight decrease, indicating that a slow reaction between dissolved gas and water occurs. The length of the induction period is known to be dependent upon the initial amounts of methane and water and the initial pressure applied,[12,18] but it is difficult to reproduce accurately.[5]

At the end of the induction period, an abrupt increase in the consumption of methane occurs which leads to the reactive phase with growth of methane hydrate particles. At this stage, macroscopic methane hydrate particles can be observed visually. The determination of the initial rate is indicated in Figure 4.

Computational Results

Figure 5A shows the result of a simulation including the induction period and the reactive phase. During the induction period methane gas is stirred into the water phase by process M1 while precursor N and hydrate H are slowly formed by processes M2 and M3.

Figure 5B shows how concentrations of dissolved methane, precursor species N, and hydrate species H vary as a function of time. During the induction period the concentration of dissolved methane approaches a steady state value which rapidly adjusts to a lower value when the growth of hydrate particles occurs in the reactive phase. The concentration of species N increases due to process M2 and due to the reverse reaction of process M4,

(18) Lingelem, M.; Majeed, A. Challenges in areas of multiphase transport and hydrate control for a subsea gas condensate production system. In *Proceedings from the 68th GPA Annual Convention*, San Antonio; Gas Processors Association: Tulsa, 1989; pp 19–29.

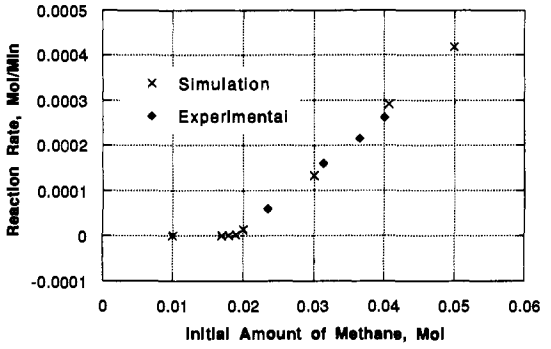

Figure 6. Computed initial reaction velocity $\Delta n(CH_4)/\Delta t$ (defined in Figure 4) as a function of the initial amount of methane compared to corresponding experiments. Conditions: initial amount of water, 14 g; temperature, 6.0 °C.

because H is being formed autocatalytically and because N and H are in a rapid equilibrium during the induction period. The end of the induction period is reached when a critical amount of N and H has accumulated. At this point fast growth of hydrate H occurs and concentration of N rapidly approaches a steady state.

The concentration of hydrate species H is very low during the induction period, but it rises suddenly at the end of the induction period; from this point on, H grows with the same rate as methane gas is consumed. The inset in Figure 5B shows hydrate growth by orders of magnitude during the induction period and growth period.

The length of the induction period is determined by the rate constant k_3 of the uncatalyzed conversion of N to H and the rate constants of the autocatalytic processes M4 and M5. In general, the length of the induction period decreases as the rate constants of processes M1, M2, and M3 increase.

The transition between the induction period and the reactive phase becomes more abrupt as k_3 and the rate constants of processes M4 and M5 differ in magnitude, i.e., as k_3 decreases and k_4 and k_5 increase.

While the rate constants k_1 and k_{-1} have been fixed to their experimentally estimated values (Table II), the remaining rate constants (Table I) were chosen to give quantitative agreement with the experiment displayed in Figure 4. In addition to this fit, which is shown in Figure 5A, we have also compared simulations using the rate constant values of Table I with experiments where the initial amount of methane is varied. Figure 6 shows that the computed reaction rates (at the beginning of the reactive phase, see Figure 4) are in very close agreement with corresponding experiments.

Discussion

The Induction Period. The reaction scheme M1–M5 represents the first set of pseudoelementary processes, which successfully and at least at a semiquantitative level simulate the presence of an induction period and the subsequent reactive phase in the formation of methane hydrate.

There have been previous proposals of molecular mechanisms, especially in describing the initial delay (induction period) of the hydrate-forming process.[5,10,15] However, these approaches have been rather qualitative in nature and none of them has included (methane) gas as an explicit kinetic variable or has formulated a valid mass balance for the reacting gas species or intermediates.[15]

In our model, the length of the induction period is dependent on the rate of buildup of nuclei N which represent an oligomeric "precursor" of the polymeric hydrate species H. During the induction period nuclei N aggregate to hydrate particles H. Because an increase in the amount of hydrate particles (H) will increase the number of sites where macroscopic growth can occur, we have represented the precipitation/growth of methane hydrate as an autocatalytic process.

When a certain critical concentration of hydrate H has accumulated during the induction period, then the autocatalytic process for formation of macroscopic hydrate particles H (reactive phase, Figure 4) begins. This abrupt transition between induction period and growth process can be illustrated by the following simplified reaction sequence:

$$G \xrightarrow{k_{I1}} H \qquad (I1)$$

$$G \xrightarrow{k_{I2}[H]} H \qquad (I2)$$

where G represents gas and H hydrate.

If one assumes that $k_{I1} \ll k_{I2}$, then the induction period t_{ind} for the coupled system I1 and I2 can be estimated from the (analytically) integrated rate equations of the chemical processes I1 and I2. One obtains:

$$t_{ind} = \frac{1}{k_{I2}[G]_0} \ln\left\{\frac{[G]_0}{(k_{I1}/k_{I2})} \frac{(1 - x_N)}{x_N}\right\} \qquad (2)$$

where $1 - x_N$ represents the molar fraction of G (gas) that has been converted to H at time t_{ind}. $[G]_0$ is the initial gas concentration at time $t = 0$. A good approximation for the induction period is obtained when $x_N = 0.99$, i.e., when 1% of G has been converted to H.

Although the model described by eqs I1 and I2 describes very nicely the abrupt transition between the induction period and the reactive phase, it is too simple to explain the magnitude of the gas consumption during the induction period and to describe the effect of gas concentration on the dynamics of the mixing process of methane gas into the aqueous phase (Figures 4 and 6).

The dynamics of model M1–M5 are too complicated to be analyzed analytically. The simulations show (Figure 5B) that the dissolved methane concentration, $[CH_4(aq)]$, is present in two steady states. One steady state is established during the induction period, while a lower steady state value is rapidly attained when the reactive phase has started. This sudden change in the steady state value at the end of the induction period indicates the "by-pass" of reactions M2, M3, and M4, and the dominance of the reactions M1 and M5, when hydrate H is formed. In the induction period, a steady state value in the dissolved gas concentration is obtained because dissolved gas is in a dynamic equilibrium between the dissolution process M1 and the subsequent slow reaction forming the intermediate species N. At this stage, the rates of processes M4 and M5 are negligible, because the concentration of hydrate H is still very low (Figure 5B). During the induction period the rate-determining step in the formation of hydrate H is process M3.

Makogon[10] and Vysniauskas and Bishnoi[12] found that the induction period is significantly reduced when the water used was from previously formed methane hydrate. This behavior is consistent with our mechanism. When methane hydrate is melted the water sample still contains sufficient *dissolved* methane hydrate species (N and H) such that macroscopic particle growth is initiated earlier compared to the situation when no N or H species are initially present. What could be residual hydrate particles above hydrate equilibrium temperatures have been observed for as long as one week by using light-scattering techniques.[19] Thus, by removing dissolved species N and H from the water sample by various treatments,[10,12] the induction period increases.

The Reactive Phase. In the beginning of the water–methane reaction, i.e., when no macroscopic hydrate particles are present,

the formation of hydrate particles H proceeds via the oligomeric precursor N. N probably consists of a variety of different species preceding the macroscopic methane hydrate form H. Since the buildup of H is represented by an autocatalytic process, the formation of H is assumed to occur from N (reaction M4), and when sufficient hydrate H has accumulated, it occurs also by the direct reaction between dissolved methane (CH_4(aq)) and water (process M5).

When a critical amount of hydrate H has accumulated, the autocatalytic production of H begins. It is process M5 that is now responsible for the main conversion of dissolved methane into hydrate. The autocatalytic formation of hydrate is now limited by the dissolution process of gaseous methane into the water phase (M1). This is the reason why at this point a second steady state with lower concentration is established. Process M1 as the rate-determining step during hydrate formation also explains the effect of stirring on reaction rate. Reaction rate constants k_1 and k_{-1} reflect the effectiveness of the stirrer and the factors (stirring rate, effective interphase area between methane gas and reacting solution)[12] which affect the transport of methane from the gas phase into the water phase.

Since in this work the phase transition is described by autocatalytic processes, variations in the shape/structure of the dissolved hydrate particles will affect the concentration of hydrate and may have a considerable effect on induction times (our calculations estimate the critical H amount to be approximately 10^{-9} M).

We find it astonishing that with this relatively simple model we are able to simulate, almost quantitatively, the form and length of the induction period, as well as reaction rates when the amount of initial methane gas is varied.

Future work will concentrate on testing this mechanism further. In this respect, hysteretic effects found when the methane–water system is exposed to temperature gradients appear of interest.[10] A detailed study of the factors that affect induction times will also be the subject of subsequent work. Another important area concerns the identification of the various oligomeric species represented here as the kinetic variable N.

Acknowledgment. The authors thank Esso Norge for financial support and Ronald L. Reed from Exxon Production Research Co. (Houston) for comments. We also thank Håkon Nordvik and Thor Martin Svartås for discussions and Malcolm Kelland for reading the manuscript.

(19) Nerheim, A. R.; Svartås, T. M.; Samuelsen, E. J. Investigation of hydrate kinetics in the nucleation and early growth phase by laser light scattering. In *Proceedings of the Second (1992) International Offshore and Polar Engineering Conference*, San Francisco; Chung, J. S., Natvig, B. J., Li, Y., Das, B. M., Eds.; The International Society of Offshore and Polar Engineers: Golden, 1992; pp 620–627.

(20) Svartås, T. M.; Fadnes, F. H. Methane Hydrate Equilibrium Data for the Methane–Water–Methanol System up to 500 bara. In *Proceedings of the Second (1992) International Offshore and Polar Engineering Conference*, San Francisco; Chung, J. S., Natvig, B. J., Li, Y., Das, B. M., Eds.; The International Society of Offshore and Polar Engineers: Golden, 1992; pp 614–619.